THz-TDS Parameter Extraction: Empirical Correction Terms for the Analytical Transfer Function Solution

JON GORECKI,[1,*], VASILIS APOSTOLOPOULOS,[2]

[1] *Optoelectronics Research Centre, University of Southampton, Southampton, SO17 1BJ, UK*
[2] *School of Physics and Astronomy, University of Southampton, Southampton, SO17 1BJ, UK*
[*] *J.Gorecki@soton.ac.uk*

Abstract:

Terahertz time-domain spectroscopy (THz-TDS) is capable of determining both real and imaginary refractive index of a wide range of material samples, however converting the TDS data into complex refractive index typically involves iterative algorithms which are computationally slow, involve complex analysis steps, and can sometimes lead to non-convergence issues. To avoid using iterative algorithms it is possible to solve the transfer function analytically by assuming the material loss is low, however this leads to errors in the refractive index values. Here, we demonstrate how the errors created by solving the transfer function analytically are largely predictable, and present a set of empirically derived equations to diminish the error associated with this analytical solution by an impressive two to three orders of magnitude. We propose these empirical correction terms are well suited for use in industrial applications such as process monitoring where analysis speed and accuracy are of the utmost importance.

1. Introduction

Terahertz Time Domain Spectroscopy (THz-TDS) is a powerful analytical technique which is able to directly provide information on the real and imaginary components of a materials refractive index, providing a vital spectroscopy technique to investigate material properties such as biological samples [1–4], semiconductor manufacturing [5], pharmaceuticals [6–9], monitoring atmospheric pollution [10], and mineral science applications [11]. THz-TDS also has been used for interrogating light-matter interactions such as plasmons [12–15], polaritons [16–18], and charge carrier dynamics [19, 20]. Future development of THz-TDS is seen to be a lucrative technology for industrial sensing and manufacturing applications [21]; however there remain several practical obstacles to overcome before mass industry uptake such as measurement speeds, accuracy of measuring layers of sub-wavelength thickness, and the speed and reliability of data analysis methods.

To extract complex refractive index from TDS data it is not possible to separate the real and imaginary components [22], and therefore to overcome this issue of non-separability various iterative fitting routines [23–26] are often used such as the Newton-Raphson (NR) method, or the Nelder-Mead method [27, 28], essentially in which an initial guess is made for the complex refractive index, passed through the transfer function, compared to the experimental data, and then the values are iteratively improved until reaching a set convergence value. Iterative approaches such as the Newton-Raphson method allow for complex values of refractive index to be obtained which match to the experimental data with a high degree of accuracy and are generally considered to be able to approach arbitrarily close to the true values. However the trade-off here is that the implementation of these methods can be computationally slow to reach a convergence, and can require the writing of complicated iterative algorithms. Although these algorithms are well documented in literature for the case of thick slab dielectric materials with

an air reference, developing such an algorithm can be challenging when custom and unusual geometries are analysed such as multi-layer coatings or thin films. Further, there may arise issues of non-convergence [22] which can lead to either incorrect refractive index values, or time-out errors when the algorithm reaches the maximum number of allowed iterations without convergence. The topic of THz-TDS analysis is too expansive to be covered here, however for a fuller overview the reader should look towards several well written reviews on this topic [29–31].

To increase the accuracy of extracted values of complex refractive index values from THz-TDS several authors have proposed further correction terms to be added to the transfer function equations. A Gouy phase shift correction can be applied to THz-TDS data to correct for the non-plane wave-front of a focused Gaussian THz beam [32,33] which has been demonstrated with 2D semiconductor materials to increase the accuracy of extracted charge carrier parameters [34]. The parameters extracted by THz-TDS are extremely dependent on an accurate independent measure of sample thickness; to this end an extraction technique has been proposed in which multiple internal pulse echos within the sample are measured and the input sample thickness varied until the extracted parameters from each echo result in the same refractive index [35]. Additionally it is possible to use these internally reflected echo pulses to self-reference the THz signal and remove the need for an independent air reference scan, which is shown to reduce variation between repeated TDS measurements [36]. Further, systematic artifacts arising from the finite response speeds of photo-conductive antenna THz detectors can lead to artificial bandwidth reduction of measured signals, however it is possible to correct these errors in the data-extraction process [37]. Additionally, in the analysis of semiconductor charge carriers a set of equations has been proposed to increase the accuracy of extracted parameters and simplify the analysis process [38]. To negate the reliance on these iterative procedures it is possible to solve the complex transfer function analytically by making an approximation of low-loss materials where n (real refractive index) $>> k$ (imaginary refractive index) which enables the real and imaginary components of the transfer function to be easily separated [30, 39]. This analytical solution (AN) enables values of refractive index to be obtained in a fast and computationally efficient manner with a few simple lines of computer code, however the values obtained by this method suffer with a low degree of accuracy, especially at low frequencies.

Here we present a method to increase the accuracy of the analytical solution by addition of several empirical correction (EC) terms, which allow for the fast computation times of the analytical solution to be maintained while increasing the accuracy of the computed values. By simulating THz-TDS data for a wide range of values of complex refractive indices and thicknesses we investigate the errors produced by the analytical solution and present a simple set of correction terms which reduce these errors. We show that the empirical correction terms are able to reduce the fractional difference between computed and actual values by an impressive two to three orders of magnitude for both experimental and simulated data (extending from 0.05 to 20 THz for simulated data). The terms presented here are created for THz-TDS in transmission mode, however similar terms could be created for reflection mode equations. We propose that these empirical correction terms are of use in high-throughput industrial applications such as THz-TDS for in-line process monitoring where speed and accuracy are of the utmost importance.

2. Developing the Empirical Correction Terms

We define an idealised material with flat parallel edges, thickness d, and a frequency varying complex refractive index $\tilde{n}_\omega$. In traditional THz-TDS measurements a THz pulse transmitted through the sample is measured in the time domain; the sample is then removed and a reference pulse is measured through air. An example of a typical THz-TDS transmission setup is provided in Figure 1(a). By performing a Fast Fourier transform (FFT) the time-domain pulses can be converted into the frequency domain, transformed into complex polar co-ordinates, and a phase unwrapping performed. Finally a normalisation process is required where the amplitude of

sample FFT is divided by the amplitude of the air reference FFT, and the phase of the sample FFT is subtracted from the phase of the air reference FFT. To extract the complex refractive index a transfer function is used which models the light-matter interaction; for a transmission measurement the transfer function is composed of two Fresnel transmission coefficients (to describe the light entering and exiting the sample) and a complex propagation term (to describe the light propagation through the sample). The transfer function for a single pass through a material slab is given in Equation 1; where d is the thickness of the sample, ω is the angular frequency, $\tilde{n}$ is the complex refractive index, c is the speed of light, and H describes the THz pulse.

$$H_{(\omega)} = \frac{4\tilde{n}}{(\tilde{n}+1)^2} exp(-i\tilde{n}\omega d/c) \tag{1}$$

The transfer function presented in Equation 1 does not have a direct solution due to the fact that the Fresnel coefficients contain real and imaginary terms which are not separable, yet to determine the material properties it is essential to find the combination of n and k which satisfy the equation. For this purpose it is customary to use an iterative fitting procedure such as the Newton Raphson method in which an initial starting guess of the values of n and k are provided and the algorithm then adjusts each value accordingly until there is a good agreement with the experimental data. This method is able to achieve highly accurate results, however there are a number of issues which can make the Newton Raphson method undesirable for implementation. Firstly, the implementation of the Newton Raphson method is laborious to write into a computer code as it requires several complicated steps which may appear rather convoluted to a 'non-expert' user, in both the coding steps and the analysis steps. The process is complicated by the existence of multiple solutions to the transfer function, and therefore it is necessary to calculate also the logarithm and the derivative of the transfer function. Secondly, due to the iterative nature of the algorithm it can be computationally slow to solve, especially when one considers that a typical TDS spectrum may contain tens of thousands of data points in the frequency domain. Finally, the Newton Raphson algorithm can sometimes suffer from non-convergence issues which results in wrong values of complex refractive index, especially when the initial refractive index values are far from the true values. If a THz-TDS system is to be deployed in an industrial setting (for example process monitoring of semiconductor or pharmaceutical manufacturing, or automobile paint-thickness monitoring) it is advantageous to look for extraction methods which are both faster to solve, and easier to troubleshoot.

One alternative to using iterative solvers is to make the assumption that the Fresnel terms in Equation 1 are completely real which then allows the real and imaginary terms of the equation to be separated and directly solved; this approximation is generally allowed when $n >> k$ which holds true for low-loss materials. The analytical solution is fast to solve and presents an intuitively easy to understand set of equations, however the computed values of refractive index suffer from a lower accuracy in comparison to the Newton Raphson and other iterative methods and the error increases rapidly at low frequencies.

In Equations 2 and 3 we present the well known analytical solution which separates the real and imaginary components of the complex transfer function (shown in Equation 1) into directly solvable equations, where Φ is the unwrapped phase and A is the magnitude of the Fourier transform.

$$exp(-i\Phi_{(\omega)}) = exp(-in_{(\omega)}\omega d/c) \tag{2}$$

$$A_{(\omega)} = \frac{4n_{(\omega)}}{(n_{(\omega)}+1)^2} exp(k_{(\omega)}\omega d/c) \tag{3}$$

From looking at Equation 2 it is intuitively understandable how this will return the wrong value of n at low frequencies as ω goes to zero the value of n will tend to zero, regardless of the true vale of n. This is because a component of the Fresnel coefficient has been removed from the equation which would not have a dependence on frequency, and would therefore correct the values at low frequencies. To attempt to correct this error we will now re-write Equation 2 to include a hypothetical unknown term S which will represent the missing term from the Fresnel coefficient, as show in Equation 4.

$$e^{-i\Phi_{(\omega)}} = S_{(n,k)} e^{-in_{(\omega)}\omega d/c} \tag{4}$$

From this point we can draw out the general shape which the correction term will take by re-arranging the equation to solve for n, where it can be predicted the correction term will be similar to $log(S_{(n,k)})/\omega d$. Generally it seems that this is as far as we can proceed along this avenue of thought as it does not appear possible to directly find an analytical solution for $S_{(n,k)}$, however we can investigate further by simulating THz-TDS data for a range of n, k, d values and investigating the associated errors to find an empirical relation for the correction term.

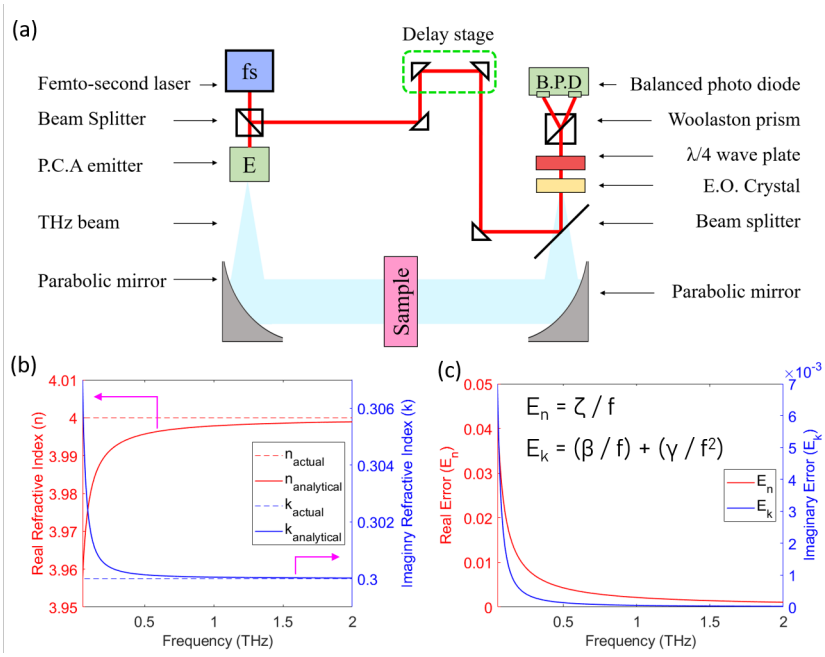

Fig. 1. **(a)** Schematic diagram of the THz-TDS setup used for experimental measurements in which a femto-second pulsed laser incident on a photo-conductive antenna emits a THz pulse, which is transmitted through a sample, and detected via an electro-optic crystal and balanced photo-diode technique. **(b)** Real and imaginary refractive index values obtained via the analytical solution to the transfer function for simulated THz-TDS data for 1 mm thick sample plotted alongside actual values, showing a large divergence at low frequencies. **(c)** The differences between calculated and actual refractive index values are plotted for real and imaginary refractive index, which are well fitted by the equations shown in the figure. The fitted lines are not shown as they overlap entirely with the plotted data points.

In Figure 1(b) we present real and imaginary refractive index values computed via the analytical solution on simulated data for a sample with $n = 4$, $k = 0.3$, $d = 1$ mm. Overlaid in the dashed lines are the actual values of real and imaginary refractive index. It can be seen that the analytical

solution is able to return fairly accurate values of refractive index at high frequencies however as the frequency decreases the values begin to diverge, where the real component tends to decrease at low frequencies, while the imaginary component increases. To investigate this effect we will describe the difference between the actual and analytical solution for the real refractive index as the 'real error' $E_n = n_{actual} - n_{analytical}$, and the 'imaginary error' $E_k = k_{analytical} - k_{actual}$.

In Figure 1(c) we plot the real and imaginary errors (E_n and E_k) against frequency where it can be seen the errors appear to follow a regular shape. In fact it is found that the real error (E_n) can be fitted extremely well by the simple function $E_n = \zeta/f$, where ζ is an unknown number. Indeed we find that when fitting E_n with this function the R^2 value of the fit is generally above 0.999. This finding is interesting as it suggests that the error associated with the analytical solution is far from random, and in reality is highly predictable. Further, this relationship agrees with the prediction we made earlier that the real refractive index obtained by AN would be missing a term with an inverse linear proportionality to the frequency. For the imaginary component the imaginary error E_k ($k_{analytical} - k_{actual}$) is found to follow the equation $E_k = (\beta/f) + (\gamma/f^2)$, where β and γ are unknown numbers. Here we propose that if the values of ζ, β, and γ are known then the errors produced by the analytical solution can be removed, allowing the user to arrive at the correct solution. We investigate further these variables with the aim to develop a set of empirical correction terms which can be applied to the values of the analytical solution to remove their systematic errors.

Focusing on the real error (E_n) the first result which is obtained is $E_n = \zeta/f$, where ζ is a variable which appears to depend on n, k and d. This dependence on frequency is a valuable first step in finding empirical correction terms as it allows us to hold frequency fixed and therefore remove one degree-of-freedom from the problem. In other words, if a value of $\zeta_{(n,k,d)}$ is found for a particular combination of n, k, d we know it will hold for any frequency. Focusing on this approach, to investigate the behaviour of $\zeta_{(n,k,d)}$ we hold the frequency constant at 0.1 THz, fix the thickness d at 1 mm, simulate data for a range of complex refractive index values, and then perform a least-squares fitting on the real error to find the variable ζ for each value of n and k. In Figure 2(a) we plot the coefficient ζ in a 3D plot against real refractive index n and imaginary refractive index k. It is noticed that ζ has a dependence on n of the general form $log(n)/n$, and is linearly proportional to k. By a trial-and-error approach it is found that the coefficient ζ can be well fitted by $\zeta = \delta \cdot k \cdot log(n)/n^{1.168}$, where n is the value of real refractive index obtained by the analytical solution, and δ is a numeric value which appears to vary with the sample thickness d.

The final step involved in determining the empirical correction term for the real component of refractive index is to explore the variable δ, where the one degree-of-freedom left to vary is the sample thickness d. By performing the previously described steps again for samples of different thickness a plot can be obtained which shows how the value of δ varies with sample thickness d. In Figure 2(b) the coefficient δ is plotted against thickness d where it is found the data is well fitted by the function $\delta = 0.0258/d$. By this approach we have now exhausted all degrees-of-freedom associated with this problem, and the final empirical correction for the real refractive index can be presented as shown in Equation 5, where the values of n and k are those obtained via the analytical solution, thickness d is quoted in millimeters, and the frequency f is quoted in THz.

$$n_{EC} = n + \frac{0.0258k}{dfn^{1.168}} log(n) \tag{5}$$

To create an empirical correction term for the imaginary refractive index a similar process is performed to find the relations of β and γ with n, k, and d. Data is simulated for a wide range of material parameters (n = 1.1 – 6) and (k = 0 – 0.5), thickness 1 mm, and the refractive index extracted via the analytical method. A fitting algorithm is used to find the values of β and γ which satisfy the equation $E_k = (\beta/f) + (\gamma/f^2)$. To investigate firstly the β term, Figure 2(c) shows the

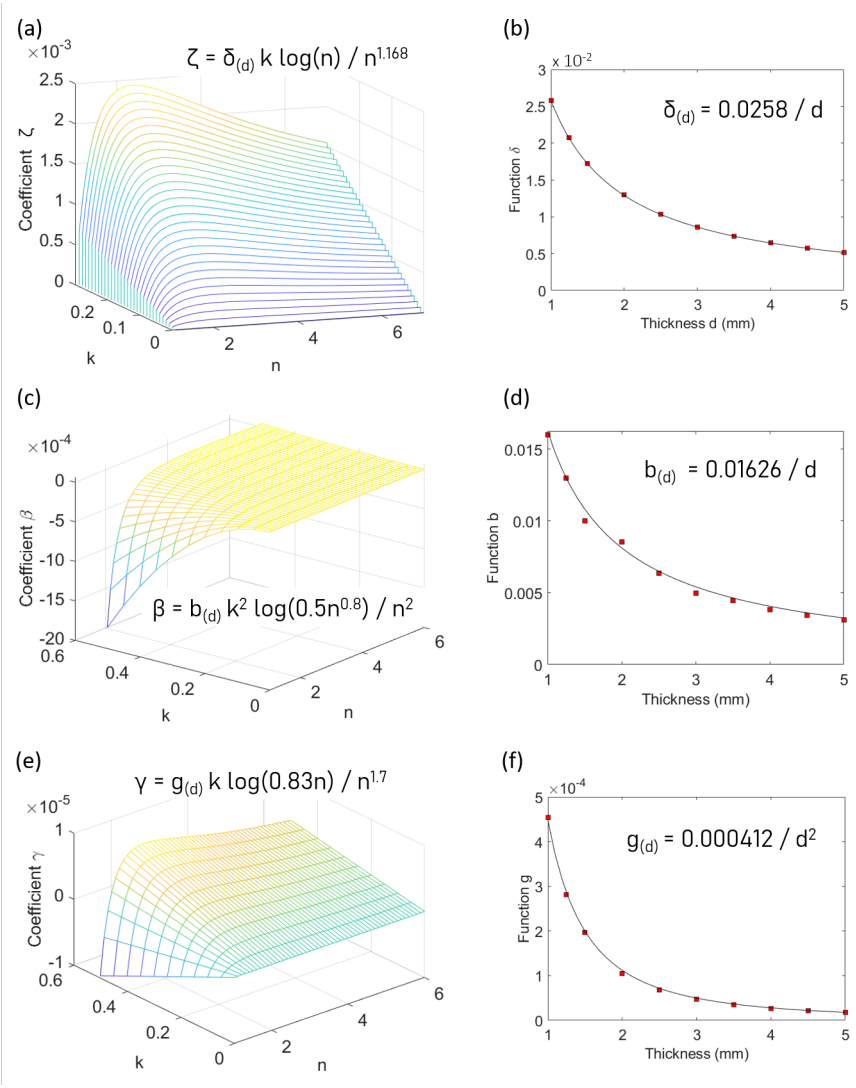

Fig. 2. To determine the coefficients for the real and imaginary errors TDS data is simulated for a 1 mm sample over a wide range of refractive index values, and a trial-and-error approach is used to obtain functions which fit well to the data. **(a)** Plot of coefficient ζ against complex refractive indices n and k, along-side **(b)** the corresponding function δ plotted against sample thickness. **(c)** Plot of the β coefficient against complex refractive index, along-side **(d)** the corresponding function b plotted against sample thickness. **(e)** Plot of the γ coefficient against complex refractive index, along-side **(f)** the corresponding function g plotted against sample thickness.

values of β plotted in a 3D graph against the values of complex refractive index at 0.1 THz. Via a trial-and-error approach it is found a generally good agreement with the data can be obtained via the expression $\beta = b_{(d)}k^2 log(0.5n^{0.8})/n^2$, where $b_{(d)}$ is a term which appears to scale with the thickness d. In Figure 2(d) we investigate this term $b_{(d)}$ by performing the previously mentioned steps for various sample thicknesses, and plot $b_{(d)}$ against d, where we find there is an inversely proportional relationship described by $b_{(d)} = 0.01626/d$. Next, in Figure 2(e) we plot on the 3D graph the values of γ against n and k and determine via a trial-and-error approach that the γ coefficient is well described by the expression $\gamma = g_{(d)}klog(0.83n)/n^{1.7}$. By running the same analysis steps for a range of thicknesses we can plot in Figure 2(f) the function $g_{(d)}$ against thickness d, and find the data points are well fitted by the equation $g_{(d)} = 4.12 \times 10^{-4}/d^2$. By putting all of these terms together we can obtain the full relationship for the empirical corrections to the imaginary refractive index as shown in Equation 6, where the values of n and k input into the equation are those obtained via the analytical method.

$$k_{EC} = k - \frac{0.01626k^2}{fn^2d} log(0.5n^{0.8}) - \frac{0.000412k}{f^2n^{1.7}d^2} log(0.83n) \tag{6}$$

3. Results and Discussion

To investigate the benefits of the empirical correction terms presented here we extract complex refractive index for experimental THz-TDS data sets for five samples; quartz (2.6 mm), fused silica (3.31 mm), PTFE (5 mm), lithium niobate (0.5 mm), and silicon (3 mm). For each of the TDS data-sets we perform a windowing operation in the time domain to remove the effects of any internal reflections within the samples, and then normalise the measurement with respect to an air reference scan. For each of the samples we extract the data with the Netwon Raphson (NR) method (where the starting values of the Newton-Raphson method were 1+0i), with the analytical (AN) method, and with the empirical correction (EC) terms. As the Newton Raphson method is able to arrive arbitrarily close to the true solution of the transfer function we will consider the refractive index values obtained by this method are the correct ones, and then compare the analytical and empirical correction methods with respect to these values. In Figure 3 we plot the refractive index of (a) quartz, (b) fused silica, (c) PTFE, (d) lithium niobate, and (e) silicon. For all five samples it can be seen that at low frequencies the analytical solution (red line) diverges from the Newton Raphson method (black line), however with the addition of the empirical correction terms (shown in the green dashed line) these values appear to fully overlap with the Newton Raphson values, which demonstrates the effectiveness of the EC terms.

In Figure 3(f) we probe further the deviation between the extraction methods; to achieve this we divide the error of the empirical correction solution ($|n_{NR} - n_{EC}|$) by the error of the analytical solution ($|n_{NR} - n_{AN}|$). By plotting the divided errors against frequency for the five material samples it can be seen that for each sample the empirical correction terms reduce the error of the extracted refractive index values. For the quartz sample there is a fairly flat behaviour which shows that across all frequencies the EC terms are able to reduce the error in refractive index by just over two orders of magnitude (or a 127 times reduction). For the fused silica sample the situation is even better where the EC terms reduce the error even further (400 times reduction). For the PTFE sample there is again a fairly uniform response over the frequency domain, where the errors are reduced by over one order of magnitude. The EC terms have the poorest performance for the PTFE sample which may be due to the low refractive index of PTFE, however there are still tangible benefits demonstrated from the EC terms. For the lithium niobate sample at high frequencies we again are able to achieve over two orders of magnitude reduction in the error by using the EC terms, however at low frequencies this tails off towards a one order of magnitude reduction. This behaviour is likely a symptom of the dispersive nature of lithium niobate where the refractive index changes rapidly below frequencies of 0.2 THz which

introduces large phase gradients in a portion of the spectrum where signal-to-noise ratio is low and therefore is highly susceptible to phase unwrapping errors, resulting in unpredictable values at low frequencies regardless of the extraction method used. Finally for the silicon sample we see a flat frequency response where the EC terms deliver around two orders of magnitude reduction in the error compared to the AN method. Our method is valid for a wide range of frequencies and although here our experimental results are limited by noise at high frequencies we find the EC method is proven to be effective on simulated data even at extremely high frequencies (up to 20 THz).

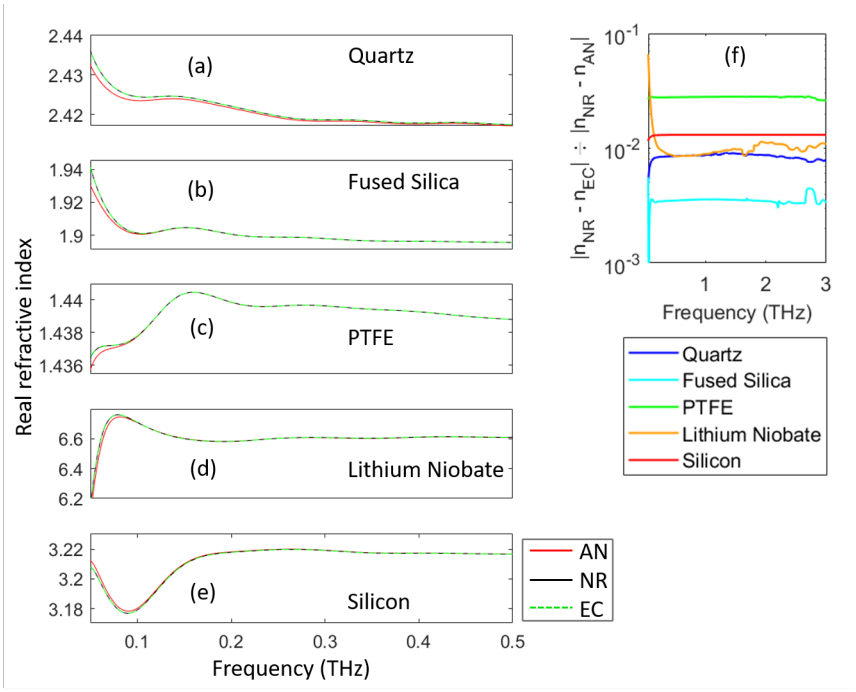

Fig. 3. The three extraction algorithms are compared for experimental data on five different material samples, where we plot real refractive index: **(a)** quartz 2.6 mm, **(b)** fused silica 3.31 mm, **(c)** PTFE 5 mm, **(d)** lithium niobate 0.5 mm, and **(e)** silicon 3 mm. **(f)** Error analysis performed by taking the absolute difference between refractive index values obtained by NR and EC methods and dividing by the difference between NR and AN methods. This comparison reveals the empirical correction terms are able to reduce the error created by the analytical solution by around two orders of magnitude for experimental data for commonly used materials.

To assess the parameter range in which the EC terms are applicable we perform a further analysis on simulated THz-TDS data for samples of 1 mm, 3 mm, and 5 mm thickness with a wide range of complex refractive index values, varying n from 1.5 to 7, and varying k from 0 to 1. We then extract the real and imaginary refractive index values by the AN and EC methods and calculate the average difference from the actual n and k values over the frequency range 0.05 to 2 THz. We then divide the average of the EC method by the average of the AN method to provide a comparative error, where a value < 1 corresponds to the EC method having a smaller error than the AN method. In Figure 4 we present this comparative error as color-maps plotted against n and k. We see from these plots that the EC method is able to work over a wide range of refractive index values and thicknesses, and can provide several orders of magnitude reduction in the error. In Figure 4(a,c,e) the differences in the real components reveal that the EC terms

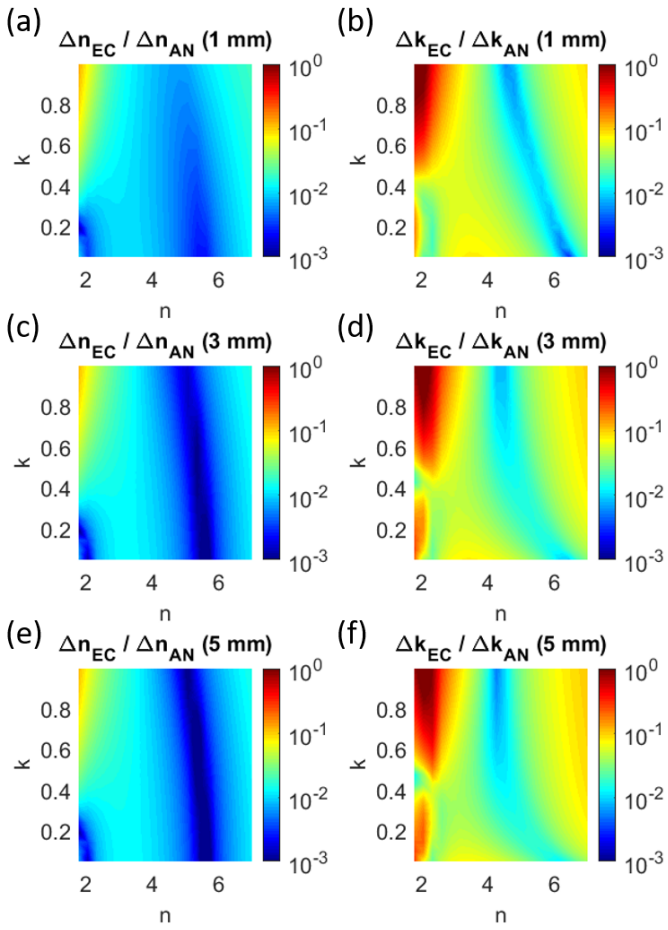

Fig. 4. Comparative study of the errors produced by the EC and AN terms for a wide range of refractive index values for simulated TDS data. Here we take the absolute difference between the refractive index obtained by the EC method and the actual value, and divide this by the difference between refractive index obtained by the AN method and the actual value. Fractional difference in **(a)** real and **(b)** imaginary refractive index for 1 mm thick sample. Fractional difference in **(c)** real and **(d)** imaginary refractive index for 3 mm thick sample. Fractional difference in **(e)** real and **(f)** imaginary refractive index for 5 mm thick sample.

provide around two orders of magnitude reduction in the error over a wide range of refractive index values. In Figures 4(b,d,f) the differences in the imaginary components are plotted for the three different sample thicknesses, where it can be seen the EC terms are still able to deliver lower errors however the improvement is slightly lower as they only achieve around 1 order of magnitude reduction in comparison to the AN method.

We find from the color-maps that the EC terms for the imaginary component starts to fail when $n = 1.5$ and $k > 0.6$, which can be observed in Figure 4(b,d,f) by the bright red patch appearing in the top left corners where the relative errors approach a value of 1, which indicates the EC and AN methods produce errors of similar magnitude. Interestingly it should be noted that it is only for the imaginary term that the EC parameter window is limited at low refractive indexes, as it can be seen in Figures 4(a,c,e) that for the real components the EC terms are effective over a much wider parameter window, which may highlight that the imaginary EC term requires further refinement in the future. Finally, by comparing the color-maps for different sample thicknesses we can see the relative improvements offered by the EC terms are fairly insensitive to sample thickness, and therefore the EC terms are generally applicable to a wide range of samples. Here we limited our minimum sample thickness to 1 mm as the analytical method to solve the THz transfer function is valid only in the case of optically thick samples where the internal reflections within the sample can be easily separated in the time domain, and as such our correction terms for the analytical solution also require an optically thick sample. The parameter space shown here was chosen as few materials exceed this parameter range, and higher k values result in such high absorption that it makes transmission mode THz-TDS a rather difficult task to complete. Therefore we conclude that the EC terms indeed cover a useful parameter window to be effective in a wide range of spectroscopy applications for both industrial and laboratory based implementations.

To provide a comparison in the computational time for the extraction methods we measure the required time for the extraction on simulated data consisting of 40960 points in the frequency domain, which is a typical resolution of a THz-TDS scan. We find the NR method to be the slowest, requiring 1.12×10^{-1} seconds, the EC method requiring 7.46×10^{-3} seconds, and the AN to be the fastest requiring 1.15×10^{-3} seconds, demonstrating that the EC method is around 15 times faster to process than the NR method. For completeness we have also investigated the Nelder-Mead method as another commonly used iterative approach however we find that this is far slower than the Newton-Raphson method and generally required around 10 times as many iterations to reach convergence.

4. Conclusion

To conclude, the complex transfer function of the THz-TDS data can be analytically solved by making the approximation that $n >> k$, however this solution diverges at low frequencies. Here we show that this error is largely predictable with a dependence on complex refractive index, frequency, and thickness. By simulating THz-TDS data for a wide range of material parameters and analysing the associated errors produced by the analytical solution we present two empirical correction terms which can be applied to the values of complex refractive index obtained by the analytical solution, which are shown to reduce the associated errors in n and k by between 2 - 3 orders of magnitude. The method presented here provides a middle-ground between the analytical solution and iterative approaches such as a Newton-Raphson method in terms of accuracy, complexity, and computation time. Further, the extraction method presented here is applicable for samples with non-uniform refractive index profiles, such as phonon-resonance features. The EC terms are appropriate for the extraction of the refractive index of bulk samples however EC terms could be similarly determined for many other measurement geometries such as thin films. We propose that this method is well suited for use in high-throughput industrial applications such as in-line process monitoring of pharmaceuticals, thickness measurements of

paint layers on automobiles, or for investigation of semiconductor materials during manufacturing, where the analysis speed and accuracy are of the utmost importance.

5. Funding

The data associated with this publication is freely available via the University of Southampton repository at eprints.soton.ac.uk/INSERT:DOI:HERE.

6. Disclosures

The authors declare no conflicts of interest.

References

1. A. Markelz, A. Roitberg, and E. Heilweil, "Pulsed terahertz spectroscopy of DNA, bovine serum albumin and collagen between 0.1 and 2.0 THz," Chem. Phys. Lett. **320**, 42–48 (2000).
2. S. Ebbinghaus, S. J. Kim, M. Heyden, X. Yu, U. Heugen, M. Gruebele, D. M. Leitner, and M. Havenith, "An extended dynamical hydration shell around proteins," Proc. Natl. Acad. Sci. **104**, 20749–20752 (2007).
3. M. Walther, B. Fischer, M. Schall, H. Helm, and P. Jepsen, "Far-infrared vibrational spectra of all-trans, 9-cis and 13-cis retinal measured by THz time-domain spectroscopy," Chem. Phys. Lett. **332**, 389–395 (2000).
4. R. M. Woodward, V. P. Wallace, R. J. Pye, B. E. Cole, D. D. Arnone, E. H. Linfield, and M. Pepper, "Terahertz pulse imaging of ex vivo basal cell carcinoma," J. Investig. Dermatol. **120**, 72–78 (2003).
5. K. Ahi, S. Shahbazmohamadi, and N. Asadizanjani, "Quality control and authentication of packaged integrated circuits using enhanced-spatial-resolution terahertz time-domain spectroscopy and imaging," Opt. Lasers Eng. **104**, 274–284 (2018).
6. C. M. McGoverin, T. Rades, and K. C. Gordon, "Recent pharmaceutical applications of raman and terahertz spectroscopies," J. Pharm. Sci. **97**, 4598–4621 (2008).
7. E. Pickwell and V. P. Wallace, "Biomedical applications of terahertz technology," J. Phys. D: Appl. Phys. **39**, R301–R310 (2006).
8. A. J. Fitzgerald, B. E. Cole, and P. F. Taday, "Nondestructive analysis of tablet coating thicknesses using terahertz pulsed imaging," J. Pharm. Sci. **94**, 177–183 (2005).
9. C. J. Strachan, T. Rades, D. A. Newnham, K. C. Gordon, M. Pepper, and P. F. Taday, "Using terahertz pulsed spectroscopy to study crystallinity of pharmaceutical materials," Chem. Phys. Lett. **390**, 20–24 (2004).
10. X. Miao, H. Zhan, K. Zhao, Z. Zhang, L. Xu, C. Zhang, and L. Xiao, "Terahertz-dependent PM2.5 monitoring and grading in the atmosphere," Sci. China Physics, Mech. & Astron. **61** (2018).
11. Y. Ma, H. Huang, S. Hao, K. Qiu, H. Gao, L. Gao, W. Tang, Z. Zhang, and Z. Zheng, "Insights into the water status in hydrous minerals using terahertz time-domain spectroscopy," Sci. Reports **9** (2019).
12. Q. Gan, Z. Fu, Y. J. Ding, and F. J. Bartoli, "Ultrawide-bandwidth slow-light system based on THz plasmonic graded metallic grating structures," Phys. Rev. Lett. **100** (2008).
13. T.-I. Jeon and D. Grischkowsky, "THz zenneck surface wave (THz surface plasmon) propagation on a metal sheet," Appl. Phys. Lett. **88**, 061113 (2006).
14. H. Yan, X. Li, B. Chandra, G. Tulevski, Y. Wu, M. Freitag, W. Zhu, P. Avouris, and F. Xia, "Tunable infrared plasmonic devices using graphene/insulator stacks," Nat. Nanotechnol. **7**, 330–334 (2012).
15. V. W. Brar, M. S. Jang, M. Sherrott, J. J. Lopez, and H. A. Atwater, "Highly confined tunable mid-infrared plasmonics in graphene nanoresonators," Nano Lett. **13**, 2541–2547 (2013).
16. S. Nishizawa, N. Tsumura, H. Kitahara, M. W. Takeda, and S. Kojima, "New application of terahertz time-domain spectrometry (THz-TDS) to the phonon polariton observation on ferroelectric crystals," Phys. Medicine Biol. **47**, 3771–3776 (2002).
17. S. Kojima and T. Mori, "Terahertz time-domain spectroscopy of raman inactive phonon-polariton in strontium titanate," Ferroelectrics **499**, 100–106 (2016).
18. S. Kojima and T. Mori, "Terahertz time-domain spectroscopy of infrared active soft mode and phonon-polariton dispersion," Ferroelectrics **500**, 183–202 (2016).
19. P. A. George, J. Strait, J. Dawlaty, S. Shivaraman, M. Chandrashekhar, F. Rana, and M. G. Spencer, "Ultrafast optical-pump terahertz-probe spectroscopy of the carrier relaxation and recombination dynamics in epitaxial graphene," Nano Lett. **8**, 4248–4251 (2008).
20. R. Ulbricht, E. Hendry, J. Shan, T. F. Heinz, and M. Bonn, "Carrier dynamics in semiconductors studied with time-resolved terahertz spectroscopy," Rev. Mod. Phys. **83**, 543–586 (2011).
21. Naftaly, Vieweg, and Deninger, "Industrial applications of terahertz sensing: State of play," Sensors **19**, 4203 (2019).
22. P. U. Jepsen, "Phase retrieval in terahertz time-domain measurements: a "how to" tutorial," J. Infrared, Millimeter, Terahertz Waves **40**, 395–411 (2019).
23. L. Duvillaret, F. Garet, and J.-L. Coutaz, "A reliable method for extraction of material parameters in terahertz time-domain spectroscopy," IEEE J. Sel. Top. Quantum Electron. **2**, 739–746 (1996).

24. L. Duvillaret, F. Garet, and J.-L. Coutaz, "Highly precise determination of optical constants and sample thickness in terahertz time-domain spectroscopy," Appl. Opt. **38**, 409 (1999).
25. T. D. Dorney, R. G. Baraniuk, and D. M. Mittleman, "Material parameter estimation with terahertz time-domain spectroscopy," J. Opt. Soc. Am. A **18**, 1562 (2001).
26. M. Scheller and M. Koch, "Fast and accurate thickness determination of unknown materials using terahertz time domain spectroscopy," J. Infrared, Millimeter, Terahertz Waves **30**, 762–769 (2009).
27. J. C. Lagarias, J. A. Reeds, M. H. Wright, and P. E. Wright, "Convergence properties of the nelder–mead simplex method in low dimensions," SIAM J. on Optim. **9**, 112–147 (1998).
28. I. Pupeza, R. Wilk, and M. Koch, "Highly accurate optical material parameter determination with THz time-domain spectroscopy," Opt. Express **15**, 4335 (2007).
29. W. Withayachumnankul and M. Naftaly, "Fundamentals of measurement in terahertz time-domain spectroscopy," J. Infrared, Millimeter, Terahertz Waves **35**, 610–637 (2013).
30. P. Jepsen, D. Cooke, and M. Koch, "Terahertz spectroscopy and imaging - modern techniques and applications," Laser & Photonics Rev. **5**, 124–166 (2010).
31. J. E. Haddad, B. Bousquet, L. Canioni, and P. Mounaix, "Review in terahertz spectral analysis," TrAC Trends Anal. Chem. **44**, 98–105 (2013).
32. V. Apostolopoulos, G. Daniell, and A. Chung, "Complex refractive index determination using planar and converging beam transfer functions," in *Terahertz Spectroscopy and Imaging,* (Springer Berlin Heidelberg, 2012), pp. 81–94.
33. P. Kužel, H. Němec, F. Kadlec, and C. Kadlec, "Gouy shift correction for highly accurate refractive index retrieval in time-domain terahertz spectroscopy," Opt. Express **18**, 15338 (2010).
34. P. R. Whelan, Q. Shen, D. Luo, M. Wang, R. S. Ruoff, P. U. Jepsen, P. Bøggild, and B. Zhou, "Reference-free THz-TDS conductivity analysis of thin conducting films," Opt. Express **28**, 28819 (2020).
35. J. Choi, W. S. Kwon, K.-S. Kim, and S. Kim, "Nondestructive material characterization in the terahertz band by selective extraction of sample-induced echo signals," J. Nondestruct. Eval. **34** (2014).
36. J. Gorecki, N. Klokkou, L. Piper, S. Mailis, N. Papasimakis, and V. Apostolopoulos, "High-precision THz-TDS via self-referenced transmission echo method," Appl. Opt. **59**, 6744 (2020).
37. E. Castro-Camus, L. Fu, J. Lloyd-Hughes, H. H. Tan, C. Jagadish, and M. B. Johnston, "Photoconductive response correction for detectors of terahertz radiation," J. Appl. Phys. **104**, 053113 (2008).
38. A. M. Ulatowski, L. M. Herz, and M. B. Johnston, "Terahertz conductivity analysis for highly doped thin-film semiconductors," J. Infrared, Millimeter, Terahertz Waves **41**, 1431–1449 (2020).
39. M. Scheller, "Data extraction from terahertz time domain spectroscopy measurements," J. Infrared, Millimeter, Terahertz Waves **35**, 638–648 (2014).